Journal of The Electrochemical Society, **153** (3) E52-E57 (2006)
0013-4651/2006/153(3)/E52/6/$20.00 © The Electrochemical Society

Convergent Iterative Constrained Variation Algorithm for Calculation of Electron-Transfer Transition States

M. Aryanpour,[z] V. Rai, and H. Pitsch*

Department of Mechanical Engineering, Stanford University, Stanford, California 94305, USA

We present an efficient mathematical framework to determine the potential-dependent transition states of electron transfer reactions by quantum calculations. This approach makes it more feasible to study heterogeneous electron transfer processes with the theory of local reaction center for electron transfer. It is shown that the new formulation regenerates previously published results obtained by the constrained variation method. Our solution algorithm replaces the constrained optimization problem defined in a multidimensional space by a single equation in terms of only one variable that is solved for in each iteration. This method leads to fast convergence, reliability, and robustness of the located transition states for more complex systems with a larger number of degrees of freedom, especially for smooth energy surfaces.
 [DOI: 10.1149/1.2160449]

Manuscript received October 4, 2005. Available electronically January 26, 2006.

Electron transfer (ET) reactions in solutions or at heterogeneous interfaces and electrodes constitute the core of chemical processes in many applications ranging from electrochemical power generation, such as fuel cells, to biological systems. Knowledge of the electrochemical steps in these processes plays a vital role in the analysis of reaction mechanisms and in understanding the chemistry involved. While quantum computations have been extensively used to investigate many non-ET reactions in the reduction steps of oxygen in fuel cells,[1,2] similar studies on ET reactions, despite their significance, need further improvement.

The theories of ET developed over the past decades[3,4] provide insight into basic electrochemical phenomena. The quadratic model of Marcus[5] for electron transfer processes has been widely applied to describing outer-sphere reactions,[6] adiabatic electron transfer at the electrode surface,[7,8] as well as nonadiabatic ET reactions.[9,10] The main challenge in dealing with ET reactions is the dependence of rate parameters, such as activation energies and frequency factors, on the properties of the environment such as solvent polarizability, reorganization energy, and in particular, the electrode potential.

The effect of these factors has been studied to some extent in the past. For instance, the role of the solvent in complex reactions has been investigated by estimating the solvent reorganization energy[11-16] and also the solvent interaction with an electric field[17] using ab initio and classical molecular dynamics simulations.

Many studies on electrochemical reactions use the Butler–Volmer approximation to describe the dependence of electrochemical reaction rates on the electrode potential. In this model, the electrode potential linearly affects the activation energy of an ET reaction. However, quantum and semiclassical theories of electron transfer processes indicate a nonlinear dependence of the activation energy on the environment parameters including the electrode potential, which are of great importance in describing ET reactions.[18] In one approach, an electron is added or removed from the whole system or a surface species to simulate the effect of charge transfer or electric field in electrochemical reactions.[19] Although this and similar techniques can provide useful information about the phenomenological trends, more sophisticated models of electron transfer are still to be incorporated into computational studies of such reactions.

In recent years, Anderson et al.[20-24] have proposed a practical approach to calculate activation energies as a function of the electrode potential using high-level ab initio quantum computations. Their model, namely, the local reaction center electron transfer theory, has been applied to investigate ET reactions such as the electrochemical oxidation of CO, the hydrogen oxidation reaction, and oxygen reduction steps both in solution and in the presence of platinum.[25-29] The above model for potential-dependent ET reactions can be applied to complex systems with a larger number of structure variables if the transition states are found with a small number of trials. In this paper, we present a new algorithm, the convergent iterative constrained variation (CICV) method, which is based on the analytical expansion of the activation energy and either the ionization potential (IP) or the electron affinity (EA) of the molecule around any local point on the potential energy surface (PES). After a brief discussion on the local reaction center theory, the new method is presented and the mathematical formulation is derived. The results obtained using this methodology for the oxidation reaction of $PtOH_2$ are compared to the literature results. Next, the CICV method is used to find the transition states of the Pt_2O_2H oxidation/reduction reactions. The results are then validated against each other based on the concept of microscopic reversibility. Finally, the convergence of this method is studied and discussed.

Local Reaction Center Theory

Historically, electron transfer processes are discussed in terms of donor and acceptor centers. In this picture, it is assumed that an electron which is initially localized in the donor region is transferred at the transition state to the distinct region of the acceptor.[3] Anderson et al.,[21-30] introduce a reaction center that instead of the conventional donor–acceptor centers in ET theories, communicates with the metal electrode. In this theory, the electron transfer state is defined as the state where the IP, for an oxidation reaction, or the EA, for a reduction reaction, of the reaction center equals the thermodynamic work function of the electrode. The work function of the electrode is in turn a function of the electrode potential E_e. Denoting EA or IP as ψ, this condition may be written for both oxidation and reduction reactions as

$$\psi = eE_e \quad [1]$$

Equation 1 expresses the ET condition in the local reaction center theory. On the scale of the standard hydrogen electrode (SHE), the electrode potential E_e is given as[29,31]

$$E_e/\mathrm{V} = U/\mathrm{V} + 4.6 \quad [2]$$

where 4.6 V is the average value of the thermodynamic work function of the SHE based on experimental estimates, and U is the electrode potential with respect to the SHE. The EA and IP of the reaction center are by definition the change in the energy when the system jumps from its initial state to its final state, i.e., the states just before and right after the charge transfer. Because the PES of the molecule is a function of multidimensional structure coordinates x for any given electrode potential, there may exist multiple configuration points on the PES that satisfy the electron transfer condition (Eq. 1). As a result, the transition state of the oxidation/reduction reactions x^* is identified as the point in the set of solutions satisfying the ET condition, where the activation energy attains its minimum.

* Electrochemical Society Active Member
[z] E-mail: aryanpour@stanford.edu

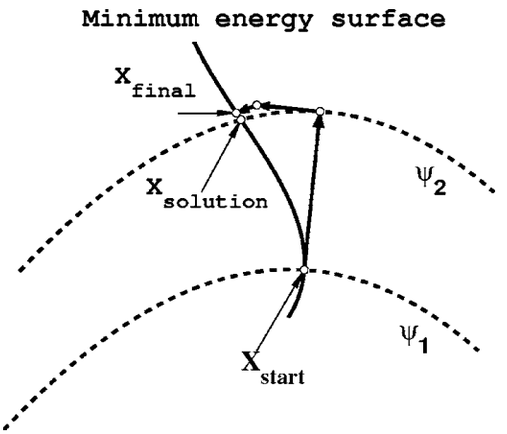

Figure 1. Graphical demonstration of the CV algorithm: the CV method locates x_{final}, which corresponds to a slightly different IP (or EA) from the target work function of the electrode ψ_2.

The activation energy at the transition state φ is the increase in the energy of the system E at the transition state with respect to the energy at the ground state

$$\varphi = E_{\text{transition state}} - E_{\text{ground state}} \quad [3]$$

In general, the dependence of the potential energy on x is not a known function, and quantum computations usually determine only sampled points on the energy surfaces. One approach that has been used to find the transition states with the above theory is the pattern search technique that compares several candidate points on the PES and picks the one with the lowest activation energy corresponding to a certain electrode potential.[23] The sampling process of the PES in the pattern search requires many quantum simulations and, therefore, is a computationally expensive solution approach.

Kostadinov and Anderson[32] used the constrained variation (CV) method, explained below, in order to reduce the number of required quantum simulations. Their approach, based on the Lagrange multipliers method, adopts a more efficient search algorithm to accelerate the determination of transition states. In this algorithm, a new variable λ is introduced to include the electron transfer condition Eq. 1 in the Lagrange function L defined by

$$L(x,\lambda) = \varphi(x) - \lambda[\psi(x) - eE_e] \quad [4]$$

The minimization of L is achieved if the partial derivatives of L with respect to all independent variables x and λ are equal to zero. This leads to the following two conditions

$$\nabla\varphi = \lambda \nabla \psi \quad [5]$$

$$\psi = eE_e \quad [6]$$

Equation 5 is a vector equality, and it demands that the gradients of φ and ψ at the transition states be colinear. The scalar Eq. 6 is the ET condition and a restatement of Eq. 1.

The computational process of the Lagrangian formulation by the CV method is carried out in two steps. In the first step, a point on the PES is found that satisfies the ET condition, i.e., Eq. 6. Next, a particular line search algorithm is followed to maintain the direction of the change in x, the structure variables, perpendicular to the gradient of ψ until the constrained minimum of φ is found by fulfilling Eq. 5 (see Fig. 1). It is assumed that the ET condition will remain the least perturbed while the algorithm simultaneously attempts to minimize the activation energy. Although the gradients of φ and ψ are calculated by finite differences using a small step size of 0.0004 Å, a shift in potential is observed as the algorithm converges to the corresponding transition states.[32] Therefore, at each step, the final transition state has an IP (or EA) that is slightly different from the target work function of the electrode (Fig. 1). Despite the substantial improvement of the CV method over the pattern search algorithm, still a large number of quantum simulations are required to compute the gradients and to find the optimum points in the multidimensional space of the configuration variables. As a result, the whole calculation time can increase tremendously if more structure variables of the nuclei configuration participate in the search algorithm.

Convergent Iterative Constrained Variation (CICV) Method

In the Born–Oppenheimer approximation, the potential energy surface of a quantum system is a function of the nuclei coordinates or, from a geometrical point of view, a function of the structure variables x. Hence, φ and ψ of the reaction center are also, by definition, functions of x. Consequently, the second-order expansions for φ and ψ within the Born–Oppenheimer approximation can be represented as truncated multivariable Taylor series about any local point on the PES

$$dx = x - x_0 \quad [7]$$

$$\psi(x) = \psi_0 + B_\psi^T dx + \frac{1}{2} dx^T A_\psi dx \quad [8]$$

$$\varphi(x) = \varphi_0 + B_\varphi^T dx + \frac{1}{2} dx^T A_\varphi dx \quad [9]$$

where A_ψ, A_φ and B_ψ, B_φ stand for the second and first derivatives of ψ and φ with respect to x evaluated at x_0

$$A_\psi = \left.\frac{\partial^2\psi}{\partial x \partial x}\right|_{x_0} \quad A_\varphi = \left.\frac{\partial^2\varphi}{\partial x \partial x}\right|_{x_0} \quad [10]$$

$$B_\psi = \left.\frac{\partial\psi}{\partial x}\right|_{x_0} \quad B_\varphi = \left.\frac{\partial\varphi}{\partial x}\right|_{x_0} \quad [11]$$

The first and second-order derivatives of the PES are available from the output of single quantum computations without performing additional calculations necessary in finite difference estimations. The gradients of ψ and φ now can be computed by taking the derivative of the above two equations with respect to x

$$\nabla\psi = B_\psi + A_\psi dx \quad [12]$$

$$\nabla\varphi = B_\varphi + A_\varphi dx \quad [13]$$

where $\nabla\psi$ and $\nabla\varphi$ are the first derivatives of ψ and φ with respect to x at any point x around x_0. The desired change dx in structure variables is then expressed in terms of the undetermined parameter λ using Eq. 5, 12, and 13

$$dx = (A_\varphi - \lambda A_\psi)^{-1}(\lambda B_\psi - B_\varphi) \quad [14]$$

Equation 14 can now be used to eliminate dx in Eq. 12 and 13. Substituting the updated expansion of $\nabla\psi$ and $\nabla\varphi$ in Eq. 6 then leads to an equation that is a function of λ only

$$\psi_0 + B_\psi(A_\varphi - \lambda A_\psi)^{-1}(\lambda B_\psi - B_\varphi) + \frac{1}{2}(\lambda B_\psi - B_\varphi)^T(A_\varphi - \lambda A_\psi)^{-T} A_\psi (A_\varphi - \lambda A_\psi)^{-1}(\lambda B_\psi - B_\varphi) = eE_e \quad [15]$$

Any root-finding algorithm such as the Newton–Raphson method can be used to solve this scalar equation for λ, which in turn directly leads to the estimation of dx from Eq. 14. Thus, the CICV method replaces the two-step multivariable approach of the CV method with a single one-variable step. The increase in the computational cost of this step with increasing the degrees of freedom of a given system is negligible and reflected only in the matrix operations of Eq. 15 and not in the quantum calculations. Therefore, the solution algorithm in the CICV method is, to a great extent, independent of the dimension of x. This is shown below.

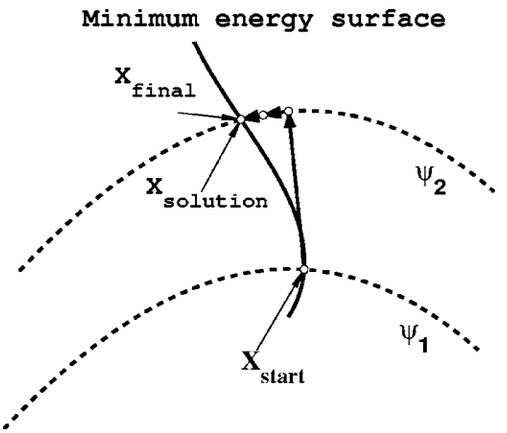

Figure 2. Graphical demonstration of the CICV algorithm: the CICV method solves the Lagrange equations such that at each iteration the IP (or EA) of the molecule converges to ψ_2.

The iteration loop begins with assigning a new value to the electrode potential starting from an initial nuclear configuration x_0. After solving Eq. 15 for λ and Eq. 14 for dx, a candidate set of structural coordinates x_1 is estimated by

$$x_1 = x_0 + dx \qquad [16]$$

Next, the EA (or IP) of the system is computed by performing two quantum simulations at the new geometry, which also provide the derivatives required for the Taylor expansions of ψ and φ in Eq. 8 and 9. The algorithm loop repeats until the cosine squared of the angle between the gradient vectors $\nabla\varphi$ and $\nabla\psi$, Eq. 17, reaches a desired value close enough to unity

$$\cos^2 \alpha = \frac{(\nabla\varphi \cdot \nabla\psi)^2}{\nabla\varphi^2 \nabla\psi^2} \qquad [17]$$

This co-linearity between $\nabla\varphi$ and $\nabla\psi$ assures the fulfillment of Eq. 5, while at the same time the solution of Eq. 15 in each iteration implies that the EA (or IP) of the reaction center is very close to the work function of the electrode.

Because this algorithm solves the Lagrange equations, Eq. 6 and 5, at each iteration, it provides more control over the electrode potential at transition states (Fig. 2). The shift in the electrode potential at transition states observed in the CV method is practically removed, because the tolerance in the target electrode potential can be set to any desired value. The number of iterations needed to locate the transition states within the accuracy of the quantum computations and of the proposed model for ET depends on the smoothness of the PES, i.e., on the precision of the second-order representation of the Hamiltonian in terms of the structure variables. Hence, for smooth energy surfaces, the CICV method converges almost independently of the dimension of the search space x. This allows a larger number of degrees of freedom in the molecule structure to be included in the constrained optimization of the system at a low computational cost, which is a valuable feature for studying larger systems.

Results

The transition states of two electrochemical reactions are presented in this paper. For the first reaction, the results obtained by the CICV method are compared with those of the CV method in the literature. In the second one, the reliability of the transition states computed by the CICV method is studied using the principle of microscopic reversibility. The convergence of the method is investigated and discussed last.

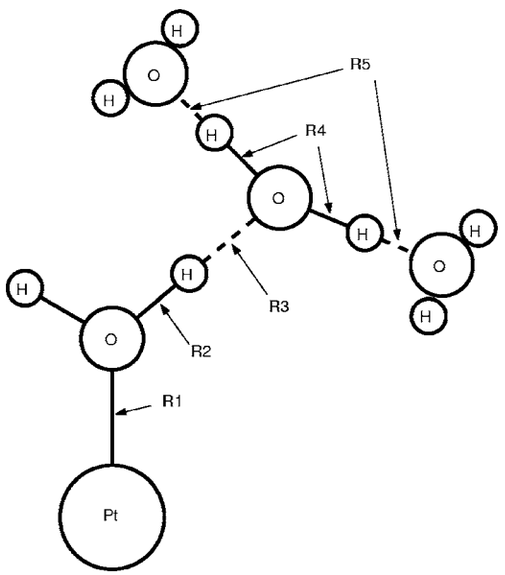

Figure 3. Reaction center for oxidation of $PtOH_2 \cdot (H_2O)_3$ along with five interatomic distances used to optimize the transition states. R4 and R5 distances were changed symmetrically for both of the two hydrogen-bonded water molecules.

Oxidation of $PtOH_2$

For comparison and demonstration purposes, the oxidation of $PtOH_2$ previously studied by Kastadinov and Anderson[32] was investigated and the activation energy vs the electrode potential was obtained using the CICV method presented in the previous section. Oxidation reactions describe the deprotonation of the adsorbed molecule according to

$$PtOH_2 \rightarrow PtOH + H^+ + e^-(U) \qquad [18]$$

The details of quantum computations, repeated here for convenience, are the same as those used by Kostadinov and Anderson.[32] The hydronium ion was modeled by a hydrogen atom attached to three water molecules, $H^+–OH_2(OH_2)_2$, as shown in Fig. 3. Five intermolecular distances were varied in the simulation whereas the other distances and angles were fixed at the optimized structure. The contribution of anions and cations was accounted for in the Hamiltonian of the system by adding a point charge of $-\frac{1}{2}e$ placed 10 Å away from the first oxygen atom of the hydronium ion along the $H^+–O$ line. This point charge corresponded to the Madelung sum for a rock salt structure of ions in a 0.1 M solution of monoprotic acid. The quantum simulations were performed using the MP2 level of theory implemented in GAUSSIAN 03[33] along with the 6–31G** basis set for O and H, and an effective core potential and double zeta valence orbital basis (LANL2DZ) set for Pt. Before the actual CICV calculation, the five distances in the reaction center were optimized while the other structure distances and angles were fixed at their corresponding ground state values. The optimized structure is equivalent to the point of zero activation energy illustrated in Fig. 4, and it serves as the starting point for the CICV computations. The calculated electrode potential at zero activation energy is 0.856 V, which is very close to the value of 0.867 V obtained in Ref. 32. Figure 4 demonstrates the potential dependence of the activation energy for the oxidation of the $PtOH_2$ precursor hydrogen-bonded to three water molecules using the CICV method. It is observed that the CICV method can reproduce the activation energy curves in very good agreement with those obtained by the CV method. The slight disagreement might be due to small differences in the optimized structure parameters.

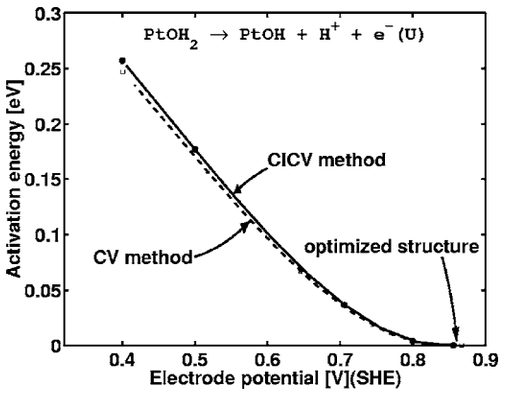

Figure 4. Activation energy at different potentials for oxidation of $PtOH_2 \cdot (H_2O)_3$ from the CICV method compared with the CV method.

Microscopic Reversibility of Pt_2O_2H Oxidation/Reduction

To further examine the accuracy of the computed transition states by the CICV method, oxidation/reduction steps of Pt_2O_2H were studied as an additional test case

$$Pt_2 - O_2 + H^+ + e^-(U) \rightleftarrows Pt_2 - O_2H \qquad [19]$$

The structure of Pt_2O_2, hydrogen-bonded to a hydronium ion (Fig. 5), constitutes the precursor for Reaction 19. Here we show that the results predicted by the CICV method satisfy the principle of microscopic reversibility, which requires that the transition configurations be the same at any electrode potential for the forward and backward reactions.[34] Microscopic reversibility offers a way to derive the oxidation curve from the reduction data and vice versa. The agreement between the calculated and the derived curves indicates the consistency of the transition states identified by the solution algorithm.

The solution algorithm locates the transition states of the oxidation/reduction steps for the molecule shown in Fig. 5. The activation energies that are computed from these transition states are called calculated activation energies. The EA of the reduced center and the IP of the oxidized center in Eq. 19, which equal to the electrode potential, are determined from the PES of the same precursors. These PES surfaces, which are determined independently

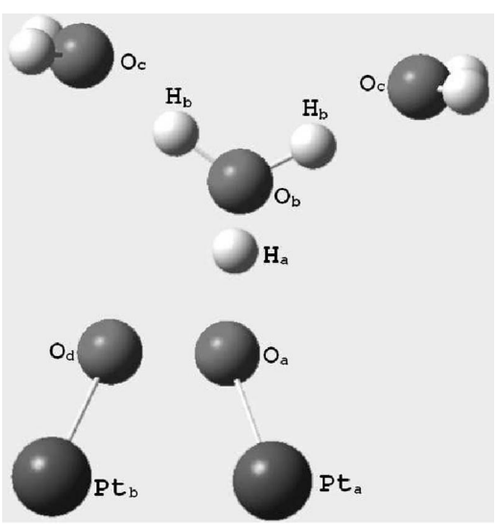

Figure 5. The reaction center for Pt_2O_2H oxidation/reduction reactions: Pt_2O_2H attached to three water molecules to account for the effect of the solution.

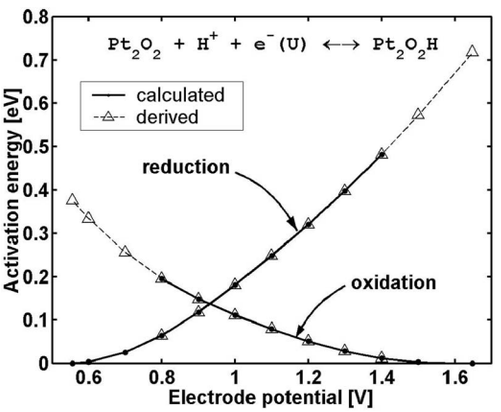

Figure 6. Calculated and derived activation energy curves for Pt_2O_2H reactions after the first series of computations using the CICV method to determine the transition states.

from both the forward and backward steps, should match in principle. Therefore, at any given electrode potential, the transition state on these PES surfaces should correspond to the same molecular structure. Having computed the transition states from one step, one can obtain the activation energies for the other step using Eq. 3. Here, these latter activation energies are called derived activation energies.

Anderson et al.[34] report difficulties in obtaining Pt_2O_2H activation energy curves in the first series of usual calculations by the CV method. Namely, the activation energies obtained by computing the reduction reaction do not match those computed from the data obtained in computing the oxidation reaction, thereby violating the principle of microscopic reversibility. This problem has not been observed for simpler systems, such as hydrogen reactions on Pt, where the transition configurations were found to be compatible for the forward and backward reactions. It was suggested to determine the true transition states of Pt_2O_2H reactions by starting the CV calculations from a structure corresponding to the average of the structures found from the computations of the oxidation and the reduction reactions.[34] Using this procedure, the activation energies obtained after three such iterations were in agreement with those determined from the data of the reverse reaction.

In contrast to the CV method, the activation energy curves from the CICV method are directly obtained in the first calculation and are in remarkable agreement with the curves derived from the reverse reactions. This is shown in Fig. 6. The requirement of microscopic reversibility is hence satisfied, which confirms the reliability of the transition states computed using the CICV method. Ten degrees of freedom were optimized in the constrained variation calculations (Table I). Varying this large number of optimization parameters, which was made possible by the new method, is the reason for observing such good agreement. The intersection point of the oxidation and reduction activation energy curves in Fig. 6 corresponds to an electrode potential of 0.93 V, which is only 0.01 V different from the value computed by Anderson et al.[34] The CICV curves for this case also compare well with the final activation energies of the CV curves, which are not shown here.

Convergence of the CICV Method

In the solution algorithm of the CICV method, the electrode potential appears as a parameter. Hence, the activation energy has to be computed for each specified value of the electrode potential. The simulations start typically with the structure of the transition state determined for the previous potential. Within the computation of the activation energy of each specified potential, several iterations may be needed to meet the convergence criteria. A simulation is considered converged if both of the convergence criteria corresponding to

Table I. Degrees of freedom of the precursor in the Pt_2O_2H oxidation reaction, Eq. 19.

DOFnumber	DOF type	Atoms[a]
1	Bond length	H_a–O_a
2	Bond length	O_b–H_a
3	Bond length	O_a–O_d
4	Bond angle	O_a–O_d–Pt_b
5	Bond angle	H_a–O_a–O_d
6	Dihedral angle	H_a–O_a–O_d–Pt_b
7	Bond length	O_d–Pt_b
8	Bond angle	O_d–Pt_b–Pt_a
9	Bond length	H_b–O_b
10	Bond length	O_c–O_b

[a] The atomic labels of the molecule are depicted in Fig. 5.

the conditions given by Eq. 5 and 6 are met. The first condition is that $1 - \cos^2 \alpha$ has to be smaller than a prescribed tolerance. The second condition demands that $|\psi/e - E_e|$ be smaller than a second prescribed tolerance.

Here, the number of iterations required to determine the activation energy for a given potential is used to assess the convergence of the CICV method for different degrees of freedom in the structure variables. The activation energy curve for the oxidation of Pt_2O_2H, given in Eq. 19 was obtained allowing for two, six, and ten degrees of freedom. These degrees of freedom are defined in Table I. For each case, eight different potentials were computed with 0.0005 as the tolerance for the $\cos^2 \alpha$-condition, and 0.01 V for the electrode potential condition.

Figure 7 shows that more iterations are needed for 6-degrees of freedom (DOF) and 10-DOF cases compared with the 2-DOF case. However, the 10-DOF case needs essentially the same number of iterations to achieve convergence as the 6-DOF system. This result is expected, because the solution algorithm is to a large extent independent of the dimension of the structure variable vector x. In each iteration, only the nonlinear scalar equation, Eq. 15, is solved for λ. Consequently, the convergence is mainly affected by the accuracy of the Taylor expansions in Eq. 8 and 9 to represent the PES of the system. This depends less on the number of structure variables than the point on the PES used as the initial guess. In principle, it could be expected that the expansion is more accurate for a smaller number of DOF, but the opposite could be the case. As an example, this can be observed for the high-potential, 10-DOF simulations, which require fewer iterations than the corresponding 6-DOF simulations.

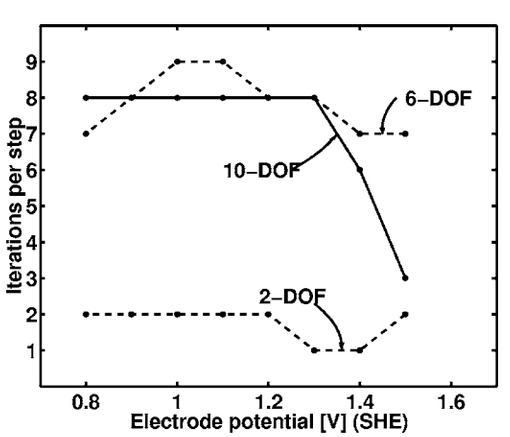

Figure 7. Number of iterations per step required for the oxidation reaction of Pt_2O_2H.

Conclusion

The CICV method is proposed to compute transition states and potential-dependent activation energies of electron transfer reactions. It is shown that the method offers faster convergence and better control over the desired electrode potential compared to the CV approach by Kostadinov and Anderson[32] and the pattern search methods. The CICV approach is a constrained optimization method using the method of Lagrange multipliers, which leads to two $(N + 1)$ conditions, where N is the number of structure variables. These conditions are combined using Taylor series expansions to a single nonlinear equation for the Lagrange multiplier. The method exploits the first- and second-order gradients of the potential energy surface, typically provided by quantum simulation packages, such as GAUSSIAN, at no extra computational cost. The calculated activation energy curve for the oxidation of $PtOH_2$ is in good agreement with the values obtained by the CV method. The CICV method was found to be convergent in the sense of satisfying the microscopic reversibility requirement, even for complex systems. This is demonstrated for oxidation/reduction reactions of Pt_2O_2H. The convergence of the method is shown to be almost independent of the DOF in the structure variables. Instead, the convergence depends on the accuracy of the second-order Taylor series expansion of the PES.

Acknowledgments

This work was supported by Honda R&D Co., Ltd., Wako, Japan. The authors are indebted to A. B. Anderson for many suggestions and helpful discussions. We also thank A. B. Anderson and Y. Cai for providing data to compare our simulation with their already published results.

Stanford University assisted in meeting the production costs of this article.

References

1. A. Michaelides and P. Hu, *J. Am. Chem. Soc.*, **123**, 4235 (2001).
2. T. Jacob, R. Muller, and W. Goddard, *J. Phys. Chem. B*, **107**, 9465 (2003).
3. M. Newton, *Chem. Rev. (Washington, D.C.)*, **91**, 767 (1991).
4. V. Balzani, *Electron Transfer in Chemistry*, Willey-VCH, Germany (2001).
5. R. Marcus, *J. Chem. Phys.*, **43**, 679 (1965).
6. R. Marcus and N. Sutin, *Biochim. Biophys. Acta*, **811**(3), 265 (1985).
7. A. Kuznetsov and W. Schmickler, *Chem. Phys. Lett.*, **327**, 314 (2000).
8. N. Hush, *J. Electroanal. Chem.*, **460**, 5 (1999).
9. S. Gosavi and R. Marcus, *J. Phys. Chem. B*, **104**, 2067 (2000).
10. S. Gosavi, Y. Gao, and R. Marcus, *J. Electroanal. Chem.*, **500**, 71 (2001).
11. X. Li, J. Tong, and F. He, *Chem. Phys.*, **260**, 283 (2000).
12. D. Matyushov and G. Voth, *J. Phys. Chem. A*, **104**, 6470 (2000).
13. C. Hartnig, P. Vassilev, and M. Koper, *Electrochim. Acta*, **48**, 3751 (2003).
14. K. Siriwong, A. Voityuk, M. Newton, and N. Rosch, *J. Phys. Chem. B*, **107**, 2595 (2003).
15. C. Hartnig and M. Koper, *J. Phys. Chem. B*, **108**, 3824 (2004).
16. J. Blumberger and M. Sprik, *J. Phys. Chem. B*, **109**, 6793 (2005).
17. C. Hartnig and M. Koper, *J. Am. Chem. Soc.*, **125**, 9840 (2003).
18. D. Dominguez-Ariza, C. Hartnig, C. Sousa, and F. Illas, *J. Chem. Phys.*, **121**, 1066 (2004).
19. Y. Wang and P. Balbuena, *J. Phys. Chem. B*, **108**, 4376 (2004).
20. A. Anderson and D. Kang, *J. Phys. Chem. A*, **102**, 5993 (1998).
21. A. Anderson and T. Albu, *Electrochem. Commun.*, **1**, 203 (1999).
22. A. Anderson, *Electrochim. Acta*, **48**, 3743 (2003).
23. A. Anderson and N. Neshev, *J. Electrochem. Soc.*, **149**, E383 (2002).
24. Y. Cai and A. Anderson, *J. Phys. Chem. B*, **108**, 9829 (2004).
25. A. Anderson, *Electrochim. Acta*, **47**, 3759 (2002).
26. A. Anderson, R. Sidik, J. Narayanasamy, and P. Shiller, *J. Phys. Chem. B*, **107**, 4618 (2003).
27. R. Sidik and A. Anderson, *J. Electroanal. Chem.*, **528**, 69 (2002).
28. A. Anderson, N. Neshev, R. Sidik, and P. Shiller, *Electrochim. Acta*, **47**, 2999 (2002).
29. A. Anderson and T. Albu, *J. Electrochem. Soc.*, **147**, 4229 (2000).
30. A. Anderson, *Electrochim. Acta*, **47**, 3759 (2002).
31. J. O. Bockris and U. M. Khan, *Surface Electrochemistry*, Plenum Press, New York (1993).
32. L. Kostadinov and A. Anderson, *Electrochem. Solid-State Lett.*, **6**, E30 (2003).
33. M. J. Frisch, G. W. Trucks, H. B. Schlegel, G. E. Scuseria, M. A. Robb, J. R. Cheeseman, J. A. Montgomery Jr., T. Vreven, K. N. Kudin, J. C. Burant, J. M. Millam, S. S. Iyengar, J. Tomasi, V. Barone, B. Mennucci, M. Cossi, G. Scalmani, N. Rega, G. A. Petersson, H. Nakatsuji, M. Hada, M. Ehara, K. Toyota, R. Fukuda, J. Hasegawa, M. Ishida, T. Nakajima, Y. Honda, O. Kitao, H. Nakai, M. Klene, X. Li, J. E. Knox, H. P. Hratchian, J. B. Cross, V. Bakken, C. Adamo, J. Jaramillo, R. Gomperts, R. E. Stratmann, O. Yazyev, A. J. Austin, R. Cammi, C. Pomelli, J. W.

Ochterski, P. Y. Ayala, K. Morokuma, G. A. Voth, P. Salvador, J. J. Dannenberg, V. G. Zakrzewski, S. Dapprich, A. D. Daniels, M. C. Strain, O. Farkas, D. K. Malick, A. D. Rabuck, K. Raghavachari, J. B. Foresman, J. V. Ortiz, Q. Cui, A. G. Baboul, S. Clifford, J. Cioslowski, B. B. Stefanov, G. Liu, A. Liashenko, P. Piskorz, I. Komaromi, R. L. Martin, D. J. Fox, T. Keith, M. A. Al-Laham, C. Y. Peng, A. Nanayakkara, M. Challacombe, P. M. W. Gill, B. Johnson, W. Chen, M. W. Wong, C. Gonzalez, and J. A. Pople, *Gaussian 03*, Revision C.02, Gaussian, Inc., Wallingford, CT (2004).

34. A. Anderson, Y. Cai, R. Sidik, and D. Kang, *J. Electroanal. Chem.*, **580**, 17 (2005).